## Book Chapter

# Functional Spectroscopy Mapping of Pain Processing Cortical Areas during Non-Painful Peripheral Electrical Stimulation of the Accessory Spinal Nerve

Janete Shatkoski Bandeira[1], Luciana da Conceição Antunes[2], Matheus Dorigatti Soldatelli[1], João Ricardo Sato[3], Felipe Fregni[4] and Wolnei Caumo[5]*

[1]Laboratory of Pain and Neuromodulation, Universidade Federal do Rio Grande do Sul (UFRGS), Brazil
[2]Department of Nutrition, Health Science Center, Universidade Federal de Santa Catarina (UFSC), Brazil
[3]Department of Mathematics and Statistics, Universidade Federal do ABC, Brazil
[4]Physical Medicine & Rehabilitation, Berenson-Allen Center for Noninvasive Brain Stimulation, Department of Neurology, Beth Israel Deaconess Medical Center, Harvard Medical School, USA
[5]Laboratory of Pain and Neuromodulation, Department of Pain and Anesthesia in Surgery, Hospital de Clínicas de Porto Alegre, Universidade Federal do Rio Grande do Sul (UFRGS), Brazil

***Corresponding Author:** Wolnei Caumo, Laboratory of Pain and Neuromodulation, Department of Pain and Anesthesia in Surgery, Hospital de Clínicas de Porto Alegre, Universidade Federal do Rio Grande do Sul (UFRGS), Porto Alegre, Brazil

Published **July 13, 2020**

This Book Chapter is a republication of an article published by Wolnei Caumo, et al. at Frontiers in Human Neuroscience in June 2019. (Bandeira JS, Antunes LC, Soldatelli MD, Sato JR, Fregni F and Caumo W (2019) Functional Spectroscopy Mapping of Pain Processing Cortical Areas During Non-painful Peripheral Electrical Stimulation of the Accessory Spinal Nerve. Front. Hum. Neurosci. 13:200. doi: 10.3389/fnhum.2019.00200)

**How to cite this book chapter:** Janete Shatkoski Bandeira, Luciana da Conceição Antunes, Matheus Dorigatti Soldatelli, João Ricardo Sato, Felipe Fregni, Wolnei Caumo. Functional Spectroscopy Mapping of Pain Processing Cortical Areas during Non-Painful Peripheral Electrical Stimulation of the Accessory Spinal Nerve. In: Prime Archives in Neuroscience. Hyderabad, India: Vide Leaf. 2020.



**Ethics Statement:** The study protocol was approved by Hospital de Clínicas de Porto Alegre Ethics Committee Board (Institutional Review Board IRB 0000921), according to the Declaration of Helsinki. All subjects provided their written informed consent. The protocol was developed in accordance with the Consolidated Standards of Reporting Trials—CONSORT, and registered at ClinicalTrials.gov (NCT 03295370).

**Author Contributions:** All authors made a significant contribution to: (a) the study concept and design, acquisition of data, or analysis and interpretation of data; (b) drafting/revising the manuscript for important intellectual content; and (c) approval of the final version to be published.

**Funding:** This research was supported by grants and material from the following Brazilian agencies: Committee for the Development of Higher Education Personnel—CAPES—PNPD/CAPES (grants to LA) and material support. Postgraduate Program in Medical Sciences at the School of Medicine of the Federal University of Rio Grande do Sul (material support). Postgraduate Research Group at the Hospital de Clínicas de Porto Alegre (FIPE-HCPA; material support). Brazilian Innovation Agency (FINEP) process number—1245/13 (to WC).

**Conflict of Interest Statement:** The authors declare that the research was conducted in the absence of any commercial or financial relationships that could be construed as a potential conflict of interest.

**Acknowledgments:** This work is dedicated to Claudio Couto MD, MsC and Grupo de Estudos de Acupuntura Neurofuncional (GEANF).

## Abstract

Peripheral electrical stimulation (PES), which encompasses several techniques with heterogeneous physiological responses, has shown in some cases remarkable outcomes for pain treatment and clinical rehabilitation. However, results are still mixed, mainly because there is a lack of understanding regarding its neural mechanisms of action. In this study, we aimed to assess its effects by measuring cortical activation as indexed by functional near infrared spectroscopy (fNIRS). fNIRS is a functional optical imaging method to evaluate hemodynamic changes in oxygenated (HbO) and de-oxygenated (HbR) blood hemoglobin concentrations in cortical capillary networks that can be related to cortical activity. We hypothesized that non-painful PES of accessory spinal nerve (ASN) can promote cortical activation of sensorimotor cortex (SMC) and dorsolateral prefrontal cortex (DLPFC) pain processing cortical areas. Fifteen healthy volunteers received both active and sham ASN electrical stimulation in a crossover study. The hemodynamic cortical response to unilateral right ASN burst electrical stimulation with 10 Hz was measured by a 40-channel fNIRS system. The effect of ASN electrical stimulation over HbO concentration in cortical areas of interest (CAI) was observed through the activation of right-DLPFC ($p = 0.025$) and left-SMC ($p = 0.042$) in the active group but not in sham group. Regarding left-DLPFC ($p = 0.610$) and right-SMC ($p = 0.174$) there was no statistical difference between groups. As in non-invasive brain stimulation (NIBS) top-down modulation, bottom-up electrical stimulation to the ASN seems to activate the same critical cortical areas on pain pathways related to sensory-discriminative and affective-motivational pain dimensions.

These results provide additional mechanistic evidence to develop and optimize the use of peripheral nerve electrical stimulation as a neuromodulatory tool (NCT 03295370 — www.clinicaltrials.gov).

## Keywords

Cortical Activation, Near Infrared Spectroscopy, Peripheral Nerve Stimulation, Electrical Nerve Stimulation, Electroacupuncture, Accessory Spinal Nerve

## Abbreviations

ACC- Anterior Cingulate Cortex; ASN- Accessory Spinal Nerve; CA- Cortical Activation; CAI- Cortical Area of Interest; DLPFC- Dorsolateral Prefrontal Cortex; EA- Electroacupuncture; fNIRS- Functional Near Infrared Spectroscopy; fMRI- Functional Magnetic Ressonance Imaging; HbO- Oxygenated Hemoglobin; HbR- Deoxygenated Hemoglobin; HRF- Hemodynamic Response Function; IMS- Intramuscular Stimulation; M1- Primary Motor Cortex; MC- Motor Cortex; NIBS- Non-invasive Brain Stimulation; NMES- Neuromuscular Electrical Stimulation; PAG- Periaqueductal Gray; PES- Peripheral Electrical Stimulation; PFC- Prefrontal Cortex; PMC- Premotor Cortex; S1/SI- Primary Somatosensory Cortex; S2/SII- Secondary Somatosensory Cortex; SMA- Supplementary Motor Area; SMC- Sensorimotor Cortex; SSC- Somatosensory Cortex; VN- Vagus Nerve

## Introduction

Pain processing physiology involves inter-related individual systems, with discriminative, affective, cognitive and social domains, leading to a magnitude of physical and emotional expressions [1,2]. Advances in neuroscience attempted to map brain areas and pathways involved in this neural network, bringing a better understanding of structural and functional brain connectivity. The prefrontal cortex (PFC) has been increasingly associated with pain processing because of its interconnections, including efferent signals to periaqueductal gray (PAG) and

dorsal horn neurons [3]. As an associative cortex, the dorsolateral prefrontal cortex (DLPFC) mediates appraisal to a rewarding stimulus, regulation of emotion and behavior and "keeping pain out of mind" function, that is, moving attention to other things rather than nociception [4]. DLPFC is also related to depression and emotional pain aspects related to anxiety [5]. Still, musculoskeletal and neuropathic pain are strongly correlated to motor cortex (MC) and its connections and has been related to pain and cognitive dysfunction by cortico-striatal-thalamo-cortical loops (CSTC; [6]). Afferent nociceptive information that crosses mediodorsal thalamus and anterior cingulate cortex (ACC) reaches DLPFC, which is related to affective-motivational aspects of pain. In turn, the sensory-discriminative dimension of pain involves spinothalamic tract pathway to ventrobasal lateral thalamus and then to sensorimotor cortex (SMC), which in turn anatomically and functionally involves MC, premotor cortex (PMC), supplementary motor area (SMA) and primary somatosensory cortex (S1; [7-9]). The importance to study the cortical processing of pain in these two target areas, nominally DLPFC and SMC, is to extend data upon the therapeutic approaches effects at the cortical level.

Peripheral electrical stimulation (PES) is being used as a non-pharmacological tool for clinical rehabilitation and treatment of pain presumably by an upward effect inducing reorganization of segmental and central networks (bottom-up outcomes; [10-12]). The postulated mechanisms include modulation of the descending modulatory system, release of peptides and endorphins at central and peripheral levels, improvement in motor recruitment, local anti-inflammatory effects, regulation of autonomic activity and changes in long-term depression (LTD)/long-term potentiation (LTP) at synaptic sites [13-15]. Neurophysiological and neuroimaging studies with PES has shown cortical hemodynamic outcomes in contralateral somatosensory cortex (SSC) and SMC to painful/non-painful type of stimulus, dependent on intensity, in the upper body (median nerve, hand or head) towards activation, using functional near infrared spectroscopy (fNIRS) devices [16-22] and functional magnetic resonance imaging (fMRI; Blickenstorfer et al., [23]). Lee et al. [24] correlated the changes

in the amplitude of the oxygenated and de-oxygenated hemoglobin with fNIRS with the pain scores on the visual analog scale (VAS) reported by volunteers after applying pain stimulus to the right thumb. Using fNIRS, neuromuscular electrical stimulation (NMES) above motor threshold with evoked pain activated contralateral SMC and bilateral PFC [25]. Aasted et al. [26] found deactivation of frontal lobe with fNIRS after applying a painful stimulus. Subsequent studies have found different patterns of activation/deactivation comparing painful to non-painful and even paresthetic stimuli using diffuse optical tomography [27,28] and fNIRS [29].

Different PES techniques are being studied to improve understanding the mechanism of action and potential indications to pain treatment. Electroacupuncture (EA) can help to treat chronic neck pain [30], chronic back pain [31] and fibromyalgia [32]. Intramuscular electrical stimulation (IMS) with needles improved pain and disability in patients with osteoarthritis [33] and chronic miofascial pain [34,35]. In previous studies using transcranial magnetic stimulation (TMS), IMS reduced the excitability of the cortical spinal pathway, decreased motor evoked potential (MEP) and intracortical facilitation (ICF) and increased current silent period (CSP; [36,37]). NMES studies have demonstrated peripheral neuromuscular adaptations such as increased muscle strength and metabolism, as well as spinal and supraspinal responses [10,23,25,38]. PES can also generate afferent signals for nerve-machine interfaces, that can be used in amputated members rehabilitation, for example [39,40]. Complementary, top-down techniques such as non-invasive brain stimulation (NIBS) are being strongly studied to successfully treat chronic pain by the application of an electrical field on central neural tissue [41,42].

Likewise, there is consistent evidence upon vagus nerve (VN) stimulation with an implantable device to aim epilepsy treatment, including potential to help to treat some neuropsychiatric conditions [43]. Using fMRI, VN transcutaneous stimulation *via* cervical and auricular sites demonstrated widespread activity in the nucleus of the solitary tract, spinal trigeminal nucleus (TN), locus coeruleus and

cortical areas [44-46]. Still, occipital and trigeminal nerve are being studied and seem to have a role on pain autonomic response and headache treatment [47-50]. Another peripheral nerve with a close connection with the VN is the accessory spinal nerve (ASN). It is the eleventh cranial nerve formed by a spinal portion from C1 to C4, and a cranial portion from nucleus ambiguous, which also forms VN [51-53]. At the level of jugular foramen, the ASN is connected to VN *via* internal ramus or *pars vagalis*. The ASN has a superficial landmark in the posterior cervical triangle and innervates the sternocleidomastoid and trapezius muscles where it receives sensory, proprioceptive and autonomic fibers *via* vagal anastomoses [54,55]. In this way, ASN can be an interesting target for its anatomical characteristics and technical facility, accessible to needles and electrodes, regarding new targets for non-invasive therapeutic interventions.

To assess cortical activation, we choose Functional Near Infrared Spectroscopy (fNIRS). It is a non-invasive neuroimaging method used to evaluate cortical function by calculating relative concentrations of oxygenated hemoglobin (HbO), de-oxygenated hemoglobin (HbR) and total hemoglobin (Total-Hb) in cortical capillary networks. Brain activity produces increased oxygen consumption, which is accompanied by increased cerebral blood flow due to neurovascular coupling, that reflects changes in HbO and HbR measurements in the observed region [56-58]. This can be interpreted as a change in tonic neural activity within that region [59]. This activity can be measured with fMRI or electroencephalography (EEG), among other techniques. FMRI has high spatial and low temporal resolution, and it is expensive; on the other hand, EEG has low spatial and high temporal resolution. The advantages of fNIRS are its low cost, portability and possibility of use during daily activities, with a plausible spatial and temporal resolution [60,61]. The main disadvantage is that it does not evaluate infracortical layers, because light has a optimal penetration-scattering rate of 2 cm deep, suffering influence of the extracerebral superficial layers [62,63]. Some authors postulate that fNIRS is a preferable tool to evaluate cortical activation induced by any type of electrical stimulation because it is less sensitive to electrical interference when

compared to other neuroimaging techniques [64]. fNIRS evaluating SSC can also be used to discriminate different stimulations, like handshake and cold temperature, as it presents different patterns of hemodynamic responses [65]. Besides that, it is being used for the development of brain-computer interfaces (BCIs; [66,67]), alone or together with others techniques as EEG [68,69].

Thus, to advance in the comprehension of the relationship between PES and the neural substrates at cortical areas involved in pain processing and understand possible therapeutic effects observed in clinical settings, this study assessed the changes on the concentration of HbO at DLPFC and SMC using fNIRS in healthy subjects that received accessory spinal nerve-peripheral electrical stimulation (ASN-PES). We tested the hypothesis that ASN-PES can promote cortical activation *via* bottom-up pathway on pain processing cortical areas modulated by top-down NIBS. Hence, this result can help to understand the clinical impact of PES on pain treatment and rehabilitation.

## Methods

The study protocol was approved by Hospital de Clínicas de Porto Alegre Ethics Committee Board (Institutional Review Board IRB 0000921), according to the Declaration of Helsinki. All subjects provided their written informed consent. The protocol was developed in accordance with the Consolidated Standards of Reporting Trials—CONSORT, and registered at ClinicalTrials.gov (NCT 03295370).

### Design Overview, Setting and Randomization

This crossover, sham-controlled clinical trial was carried out at Clinical Research Center of Hospital de Clínicas de Porto Alegre, Brazil. Healthy male volunteers, aged between 20 and 55 years, were recruited from the local community to undergo unilateral ASN-PES to evaluate cortical activation with fNIRS. Twenty-one right-handed, healthy male volunteers were eligible and agreed to participate. A standard screening questionnaire and a written consent was applied. Subjects could not have clinical

co-morbidity, chronic pain, cerebral implants, history of neurologic or psychiatric disorders, BDI-II depression scale 12 or more and no drugs or alcohol abuse. Participants were instructed not to take analgesics, anti-inflammatory drugs, caffeine or any stimulant drinks at least 6 h prior to the intervention. The randomization plan to initiate the experiment in active or sham intervention was generated by specific software[1]. Six participants were excluded, three because of exclusion criteria application and three because they did not complete recording data due to technical problems with quality of signal on fNIRS calibration before starting the procedure. After a minimum interval of 6 days, participants were crossed-over to the second intervention. The study flow is represented in Figure 1.

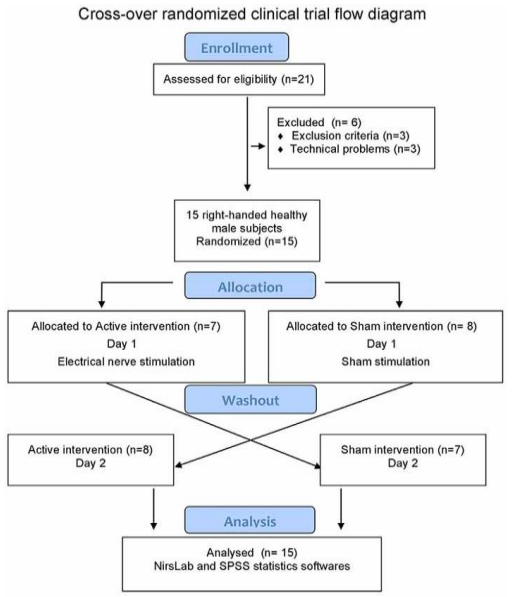


**Figure 1**: Flow diagram.

For sample size estimation (minimum 12 subjects), we performed a internal pilot study with five subjects considering an effect size on changes on the concentration of HbO related to ASN stimulation equal to 0.8 for a standard deviation equal to

6.2 (error type II of 80% and error type I lower than 5%; Birkett and Day, [70]). The power of the initial estimative was confirmed at study end.

## Assessment of Demographic and Clinical Variables

Demographic data were assessed by a standard questionnaire. Beck II Depression Inventory (BDI-II) and Strait-Trait Anxiety Inventory (STAI) evaluated depressive and anxiety symptoms, respectively. The Pittsburgh Sleep Quality Index (PSQI) assessed sleep pattern.

## Assessment of Cortical Activation

Cortical activation was assessed by fNIRS. We used a NIRx® continuous waveform NIRScout 16 × 24 device, sampling rate of 3.91 Hz, dual-wavelength LED sources (760 nm and 850 nm), differential pathlength factor (DPF) of 7.25 for WL1 and 6.38 for WL2, for a distance between sources and detectors of 3 cm, as suggested by literature to evaluate cortical layers [71,72]. Software equipment used was NIRStar 14.2 and nirsLAB 2017[2]. The montage intended to use as many channels (source-detector combination) as possible to cover motor and dorsolateral pre-frontal cortical bilateral areas, with a total of 40 measurement channels (Figure 2).

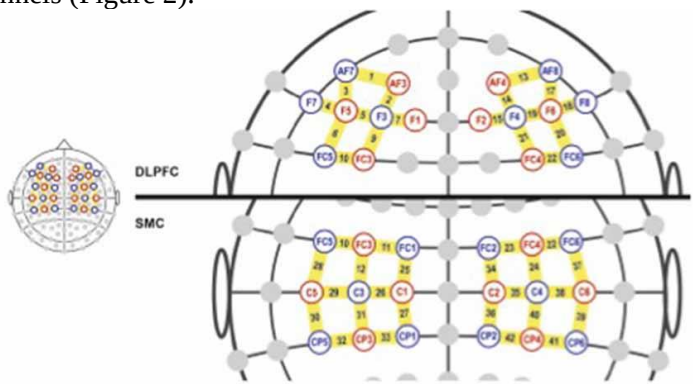


**Figure 2**: Cap montage. Sources (red), detectors (blue), in correspondence with 10/10 electroencephalography (EEG) system. Channels formed are in yellow bar. Dorsolateral prefrontal cortex (DLPFC) and sensorimotor cortex (SMC) areas are shown separately.

## Intervention

Subjects were seated on a comfortable reclining chair and asked to avoid any unnecessary movements. After the placement of the cap and software calibration checks, the signal was recorded for 10 min in resting state to surrounding accommodation. The right ASN was needled subcutaneously, at the right lateral cervical region, and the 0.25 × 40 mm sterilized acupuncture needle was fixed to the stimulator by a cable. A 12-min active or sham stimulation period was undertaken (720 s), followed by another 10 min resting-state period (Figure 3).

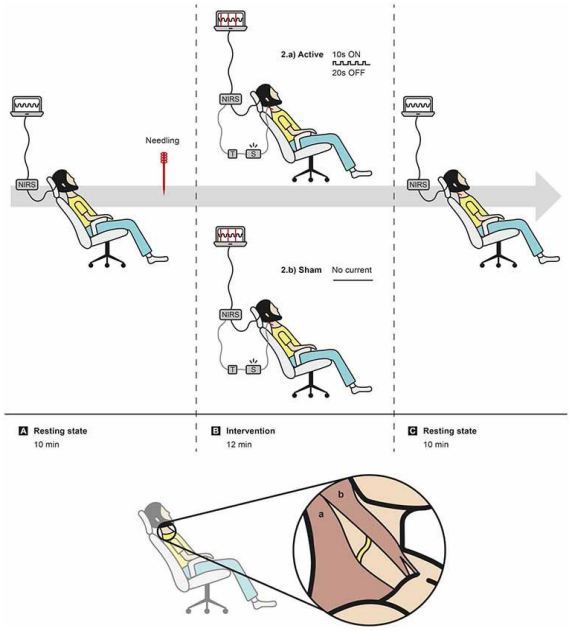


**Figure 3**: Experiment layout. Sequence of events: **(A)** 10 min of data acquisition in resting state, followed by needling right accessory spinal nerve (ASN); **(B)** randomization in active or sham intervention; **(C)** 10 min of data acquisition in resting state. In caption, representation of the subcutaneous location of the ASN (yellow trace) between trapezius muscle (a) and sternocleidomastoid muscle (b).

Electrical stimulation was undertaken with an EA stimulator (NKL 608®, made in Brazil) configured to apply a burst

rectangular 200 μs-width current with maximum 5 mA of intensity on the needle. A special trigger marker device was developed to mark in registered data the exact moment the electrical current was discharged to the subject.

The active intervention consisted of 10 Hz electrical non-painful stimulus in burst current, 10 s ON and 20 s OFF, for 12 min, generating 24 blocks of hemodynamic curves in response to electrical current on unilateral right ASN. The intensity was determined during the first 2 min according to subject tolerance, in order to get mild or moderate muscular contraction of the right superior trapezius muscle for 10 s, followed by its relaxation for 20 s. In sham procedure, the intensity button was fixed on zero and there was no muscle contraction over the 12-min period, although it was previously provoked for the localization of ASN on needling phase. Thus, sham intervention had a very small electrical stimulation period (3–5 s).

A physician researcher with more than 10 years of needling experience conducted the study. The participants were not informed of intervention type on either day. At the end of each day of intervention, the subject filled a standard adverse effects questionnaire, adapted to the particularities of EA and fNIRS devices.

Based on Jurcak et al. [73] and Koessler et al. [74], validation of spatial resolution of scalp surface and its correlation with 10/10-system EEG parameters and Brodmann's area, channels were grouped into four cortical areas of interest (CAI): left DLPFC, right DLPFC, left SMC and right SMC. Table 1 shows an approximate correlation of 10/10-system and cortical gyrus below, according to these authors. Note that the area called MOTOR includes sensory cortical zone, so it refers to SMC.

**Table 1**: Approximate anatomical correlation of international 10/10 EEG system and cortical gyrus ($n$ = 40 channels).

| | | |
|---|---|---|
| **DLPFC** | | |
| *10/10 system* | *10/10 system* | *Cortical lobe (gyrus)–Brodmann area* |
| AF3–AF7 | AF4–AF8 | Superior frontal BA 9–middle frontal BA 10 |
| AF3–F3 | AF4–F4 | Superior frontal BA 9–middle frontal BA 8 |
| F5–AF7 | F6–AF8 | Middle frontal BA 46–middle frontal BA 10 |
| F5–F7 | F6–F8 | Middle frontal BA 46–inferior frontal BA 45 |
| F5–F3 | F6–F4 | Middle frontal BA 46–middle frontal BA 8 |
| F5–FC5 | F6–FC6 | Middle frontal BA 46–precentral frontal BA 6 |
| F1–F3 | F2–F4 | Superior frontal BA 6–middle frontal BA 8 |
| FC3–F3 | FC4–F4 | Middle frontal BA 6–middle frontal BA 8 |
| FC3–FC5 | FC4–FC6 | Middle frontal BA 6–precentral frontal BA 6 |
| **SMC** | | |
| *10/10 system* | *10/10 system* | *Cortical lobe (gyrus)–Brodmann area* |
| FC3–FC5 | FC4–FC6 | Middle frontal BA 6–precentral frontal BA 6 |
| FC3–FC1 | FC4–FC2 | Middle frontal BA 6–superior frontal BA 6 |
| FC3–C3 | FC4–C4 | Middle frontal BA 6–postcentral parietal BA 123 |
| C1–FC1 | C2–FC2 | Precentral frontal BA 4–superior frontal BA 6 |
| C1–C3 | C2–C4 | Precentral frontal BA 4–postcentral parietal BA 123 |
| C1–CP1 | C2–CP2 | Precentral frontal BA 4–postcentral parietal BA 7 |
| C5–FC5 | C6–FC6 | Postcentral parietal BA 123–precentral frontal BA 6 |
| C5–C3 | C6–C4 | Postcentral parietal BA 123–postcentral parietal BA 123 |
| C5–CP5 | C6–CP6 | Postcentral parietal BA 123–supramarginal parietal BA 40 |
| CP3–C3 | CP4–C4 | Inferior parietal BA 40–postcentral parietal BA 123 |
| CP3–CP5 | CP4–CP6 | Inferior parietal BA 40–supramarginal parietal BA 40 |
| CP3–CP1 | CP4–CP2 | Inferior parietal BA 40–postcentral parietal BA 7 |

*Adapted from Koessler et al. (2009).*

## Data Processing and Statistical Analysis

While filtering and preparing the raw data, only the 12-min stimulation period was analyzed to observe the acute effects of electrical nerve stimulation on cortical hemodynamic response.

Optical density changes recorded by the software was checked for quality and continuity; channels were considered adequate in a gain setting of 7 or less and coefficient of variation of 7.5% or less to improve the signal-to-noise ratio. To calculate HbO/HbR concentration changes using modified Beer-Lambert law, data were pre-processed with default band pass filters (low cut-off 0.01 Hz; high cut-off 0.2 Hz; Scholkmann et al., [57]). For each channel, the software computed the mean amplitude for hemodynamic response averaging the measurements of 10 s of stimulation from the baseline period, that is, before stimulus.

As fNIRS devices calculate the concentration changes of HbO/HbR in millimoles per liter (mmol/l or mM) in relative proportion related to a measured baseline, the synchronization of the electrical stimulation made by the trigger marker in recorded signals was essential to correct interpretation of data, since the peak of the standard hemodynamic response function (HRF) curve is 2–6 s from the stimulus onset. In our analysis, we used HbO relative concentration changes, since it is the most sensitive parameter of activity-dependent changes in optical measurements, compared to HbR and total hemoglobin [16].

Data analysis was made by nirsLAB software by NIRx® Technologies, using a general linear model (GLM) with the standard canonical HRF pattern, and statistical parametric mapping (SPM) Student's *t*-test corrected for multiple comparisons, for the single subject level and for the group level. GLM coefficients were estimated by equation $Y = X\beta + E$, where $Y$ is the matrix of hemodynamic data; $X$ is the design matrix; $\beta$ is the GLM-coefficient matrix and $E$ is the residual term. We used GLM parameters with no pre-whitening type of analysis, where the designed matrix used rest/stimulus to generate contrast 0/1 (nirsLAB 2017 manual[3]; Tak and Chul Ye, [75]).

Shapiro-Wilk test was used to evaluate normal distribution of the variables, and Student's *t*-test was applied to evaluate differences between groups in parametric data. Multivariate analysis of covariance (MANCOVA) was used to assess statistical differences on multiple continuous dependent variables to verify

differences regarding the activation of right and left DLPFC and right and left SMC areas. Comparisons were performed using a generalized estimating equation (GEE) model, followed by the Bonferroni correction for *post hoc* multiple comparisons. We analyzed the differences in HbO concentration changes by linear regression coefficients [75], using SPSS version 22.0 (SPSS, Chicago, IL, USA). For all statistical analysis, the significance was set at $p < 0.05$.

## Results

Fifteen healthy right-handed male volunteers, mean 34.27 years old (±8.09), completed the 2-day study protocol. Demographic characteristics at baseline are shown in Table 2. No significant difference was found between groups that started with active or sham procedure on Day 1.

**Table 2**: Demographic characteristics between groups at baseline ($n = 15$).

| | Active ($n = 7$) | Sham ($n = 8$) | *p*-value |
|---|---|---|---|
| Age (years) | 36 (2.64) | 32.75 (3.23) | 0.458 |
| Education (years) | 19.43 (1.92) | 19.5 (0.96) | 0.973 |
| Body Mass Index—BMI | 26.6 (1.28) | 24.1 (1.26) | 0.186 |
| Alcohol consumption (≤1 week) | 6/7 | 6/8 | – |
| Caffeine intake before intervention (h) | >6 | >6 | – |
| State-Anxiety Inventory (STAI) | 22 (2.49) | 19.75 (1.28) | 0.420 |
| Trait-Anxiety Inventory (STAI) | 18.14 (1.45) | 17.87 (1.29) | 0.892 |
| Beck Depression Inventory (BDI-II) | 4.86 (1.62) | 2.25 (1.05) | 0.190 |
| Pittsburgh Sleep Quality Index (PSQI) | 4.29 (0.86) | 3 (0.75) | 0.281 |

*Comparisons using Student's t-test for independent samples. Results are presented in mean and standard error.*

Minimal stress and/or mild muscular tension were reported before the experiment in some subjects ($n = 5$ in active and $n = 8$ in sham), without any major clinical manifestation. Four subjects complained of minimal to mild headache or cervical pain in both

active and sham procedure, however, they were not able to distinguish if it was related to the fNIRS equipment (cap and optodes contact) or to the electrical stimulation *per se*. Prickling, itching, burning and/or heat sensation was mentioned by three subjects, related to the cap and optodes. The major discomfort mentioned was pain in the scalp, due to the tight cap and the pressure exerted by the optodes ($n$ = 9 in active and $n$ = 10 in sham). Somnolence was the most commonly reported symptom (24/30) in both active ($n$ = 14) and sham ($n$ = 10) procedures. The intensity of electrical current during active intervention required to get non-painful muscle contractions were minimal, as nerves need less electrical current to depolarize (1.133 mA ± 0.86). The electrical stimulation was well tolerated and asserted as non-painful by the participants. No relevant clinical complaint was observed.

We analyzed HbO concentration changes obtained in 30 experiments, 40 channels each, divided into active and sham group and into four CAI: left DLPFC, right DLPFC, left SMC and right SMC. The multiple dependent variables on MANCOVA model on CAI in active and sham groups are shown in Table 3. The effect of ASN electrical stimulation on HbO concentration changes was observed through the activation of right DLPFC ($F$ = 5.572; $p$ = 0.025) and left SMC ($F$ = 4.542; $p$ = 0.042) during the 10 s period of stimulation, compared to the 20 s period of rest, in active group but not in sham group. Regarding the activation of left DLPFC ($F$ = 0.266; $p$ = 0.610) and right SMC ($F$ = 1.943; $p$ = 0.174), there was no statistical difference between groups.

**Table 3**: Oxygenated Hemoglobin (HbO) concentration changes on Cortical Area of Interest (CAI) between groups ($n$ = 15).

| Dependent variable | | Type III Sum of Squares | df | Mean Square | F | p | Partial Eta Squared |
|---|---|---|---|---|---|---|---|
| Left DLPFC | Corrected Model | $1.587\ 10^{-9}$[a] | 1 | $1.587\ 10^{-9}$ | 0.266 | 0.610 | 0.009 |
| Right DLPFC | | $3.455\ 10^{-8}$[b] | 1 | $3.455\ 10^{-8}$ | 5.572 | 0.025 | 0.166 |
| Left SMC | | $5.001\ 10^{-8}$[c] | 1 | $5.001\ 10^{-8}$ | 4.542 | 0.042 | 0.140 |
| Right SMC | | $1.076\ 10^{-8}$[d] | 1 | $1.076\ 10^{-8}$ | 1.943 | 0.174 | 0.065 |
| Left DLPFC | Intercept | $2.018\ 10^{-8}$ | 1 | $2.018\ 10^{-8}$ | 3.382 | 0.077 | 0.108 |
| Right DLPFC | | $2.131\ 10^{-8}$ | 1 | $2.131\ 10^{-8}$ | 3.437 | 0.074 | 0.109 |
| Left SMC | | $2.510\ 10^{-8}$ | 1 | $2.510\ 10^{-8}$ | 2.280 | 0.142 | 0.075 |
| Right SMC | | $3.190\ 10^{-8}$ | 1 | $3.190\ 10^{-8}$ | 5.763 | 0.023 | 0.171 |

*Univariate Tests: F tests the effect based on linearly independent pairwise comparisons among the estimated marginal means. Test of Between-Subjects Effects; Multivariate Tests Observed Power = 1, 0.* [a]*R Squared = 0.009 (Adjusted R Squared = −0.026);* [b]*R Squared = 0.166 (Adjusted R Squared = 0.136);* [c]*R Squared = 0.140 (Adjusted R Squared = 0.109);* [d]*R Squared = 0.065 (Adjusted R Squared = 0.031).*

The representation of DLPFC and SMC activation between active and sham groups during ASN-PES are showed in Figures 4, 5, respectively, with mean HbO concentration changes in millimoles per liter (mmol/l), standard error of the mean (SEM) and correspondent *p*-value. Figures 6–8 show different representations of the same results found in statistical analysis. Additional data from each channel are available at Supplementary Material section. In HbO mean curves for each cortical area of interest shown in Figure 7, note that the 10 s stimulation time has a different pattern than the subsequent rest period.

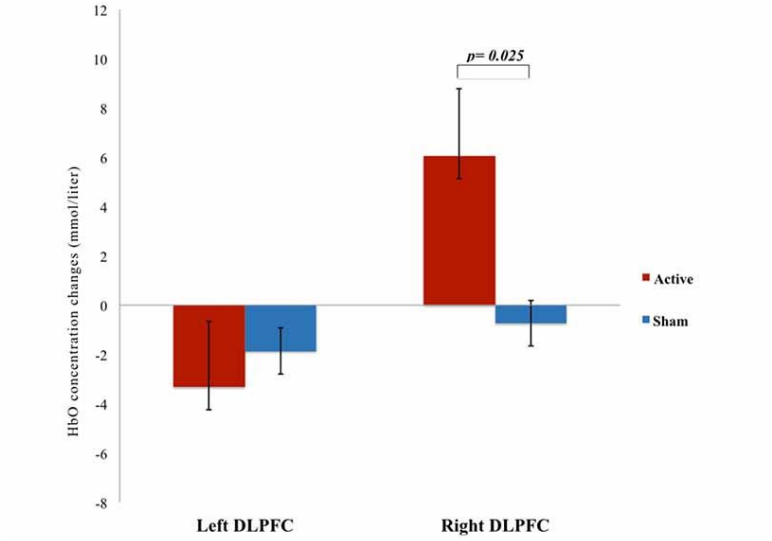


| | Mean | | SEM | | *p* |
|---|---|---|---|---|---|
| | Active | Sham | Active | Sham | |
| Left DLPFC | -3.321 | -1.866 | 2.662 | 0.932 | 0.610 |
| Right DLPFC | 6.059 | -0.728 | 2.721 | 0.928 | 0.025 |

*Bars indicate the mean and the standard error of the mean (SEM). Comparisons were performed using a generalized estimating equation (GEE) model, followed by the Bonferroni correction for post hoc multiple comparisons.*

**Figure 4**: Comparison of DLPFC activation between active and sham groups (*n* = 15). The figure shows a representation of the mean oxygenated hemoglobin (HbO) concentration changes, measured in millimoles per liter (mmol/l) with correspondent *p*-value, indicating the difference of right DLPFC activation during accessory spinal nerve-peripheral electrical stimulation (ASN-PES).

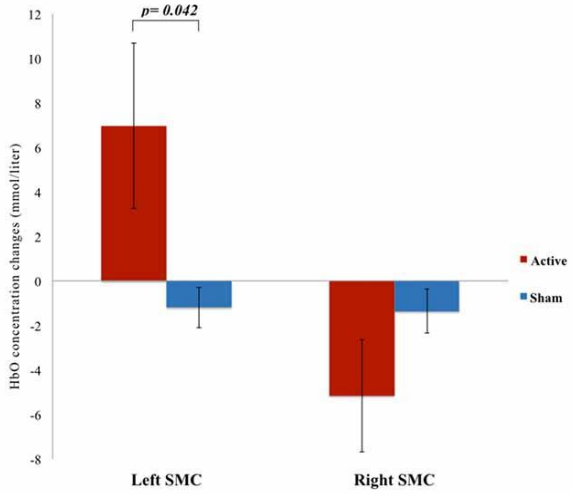


| | Mean | | SEM | | *p* |
|---|---|---|---|---|---|
| | Active | Sham | Active | Sham | |
| Left SMC | 6.976 | -1.190 | 3.721 | 0.914 | 0.042 |
| Right SMC | -5.154 | -1.367 | 2.532 | 0.984 | 0.174 |

*Bars indicate the mean and the standard error of the mean (SEM). Comparisons were performed using a generalized estimating equation (GEE) model, followed by the Bonferroni correction for post hoc multiple comparisons.*

**Figure 5**: Comparison of SMC activation between active and sham groups ($n$ = 15). The figure shows a representation of the mean HbO concentration changes, measured in millimoles per liter (mmol/l) with correspondent $p$-value, indicating the difference of left SMC activation during accessory spinal nerve-peripheral electrical stimulation (ASN-PES).

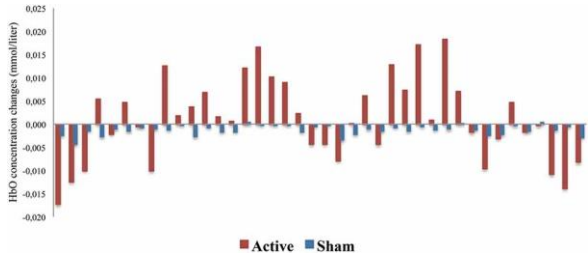


**Figure 6**: HbO concentration changes in each channel between active and sham groups ($n$ = 40). The figure shows a representation of the mean HbO concentration changes, measured in millimoles per liter (mmol/l), in each channel, demonstrating subtle changes in oxy-hemoglobin between active and sham groups in almost all of 40 channels.

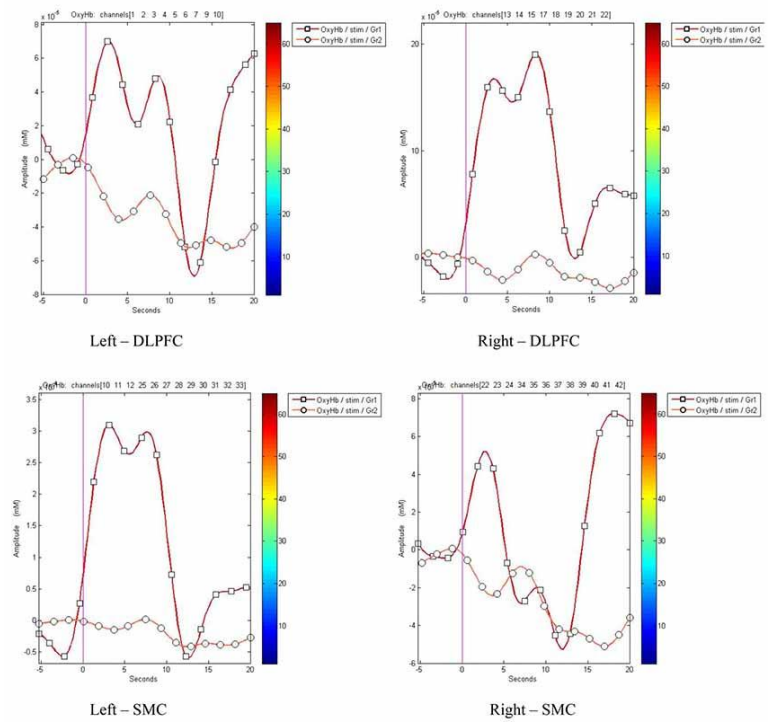


**Figure 7**: HbO mean curves for each cortical area of interest between groups. Channels were gathered to display the oxy-hemoglobin changes for active (Gr1) and sham (Gr2) groups, from 5 s before (baseline) to 20 s after stimulation onset.

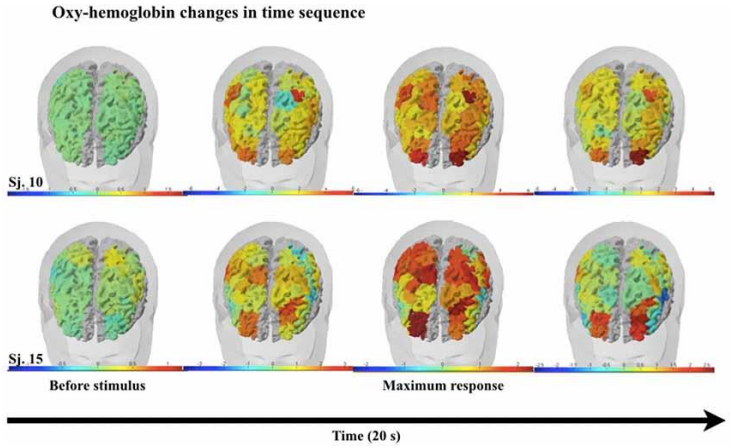


**Figure 8**: Graphic representation frames on a 3D brain surface model in two subjects, showing oxy-hemoglobin changes in time sequence. Color bars represent activation (red) or deactivation (blue) response. The first frame represents oxy-hemoglobin before the electrical stimulus, followed by frames in time sequence.

## Discussion

This study confirms our hypothesis that the ASN-PES can promote cortical activation on areas involved in pain and emotion, nominally SMC and DLPFC. Our findings showed that unilateral right ASN electrical burst stimulation with 10 Hz 10 s ON and 20 s OFF was able to activate ipsilateral dorsolateral prefrontal (DLPFC) and contralateral sensorimotor (SMC) cortical areas during stimulation. ASN-PES induced changes in regional cerebral blood flow in central pain-related regions, significantly increasing the perfusion in those areas in active but not in sham stimulation. Thus, it was able to produce bottom-up activation to central brain regions of pain processing.

The relevance of these results is to extend literature upon PES effects to modulate cortical areas involved in pain processing and help to investigate neurobiological mechanisms of peripheral neuromodulatory techniques. Furthermore, it helps to understand systemic effects observed in clinical practice and supports the possibility of using this type of non-painful peripheral stimulation as a therapeutic approach in pain treatment,

including the possibility to use combined methods to induce a top-down (e.g., NIBS or behavioral therapies) and bottom-up modulation (e.g., dry-needling). It also allows more understanding on pain mechanisms considering its dimensions, which comprises sensory-discriminative, affective-motivational and cognitive-behavioral aspects [1], as these manifestations are linked to neural networks of SMC and DLPFC.

Regarding the activation of SMC, our work is lined up to previous results in the literature and suggest that the temporal resolution of fNIRS offers an efficient technical solution to study the cortical areas activated by PES. However, in left DLPFC and right SMC, we did not find statistical difference between baseline and 10 s stimulation, but we observe that there is a subtle rise in HbO concentration towards activation on subsequent 10 s of rest, as shown in Figure 7. Although it can be associated to an error type, another hypothesis is that these areas are also activated, with a temporal delay, in active but not in sham group. Another hypothesis is that some targets areas are activated in detriment of deactivation of others. Indeed, temporal changes were found by others authors, as decrease of cortical activation during execution of hand movements using fNIRS after 5 min of electrical stimulation [64]. Besides that, parts of activated circuits and subsequent temporal responses seem to be enrolled by inter-hemispheric functional connections [76]. Furthermore, different functions of the right and left hemispheres, right and left DLPFC and medial and lateral PFC sub-regions in pain processing and in unpleasant sensations are involved in neural networks not yet clarified [77-79].

This study added value to the fact that ASN-PES is **non-painful** and utilize intensities above motor threshold. The goal of ASN needling is not to cause pain in the subcutaneous insertion of the needle in the cervical region, tangentiating the nerve to get its depolarization. The electrical current must flow through the perinervous layer, without hurting the nerve tissue. This causes mild to moderate movement of the muscles under ASN domain, i.e., trapezius muscle and sometimes sternocleidomastoid muscle, without pain. It has the same goal as functional electrical stimulation (FES), where a non-painful electrode stimulus

generates action potentials resulting in contraction of the target muscles. In Blickenstorfer et al.'s [23] study with FES, fMRI showed activation pattern in the contralateral M1, S1, PMC and the ipsilateral cerebellum, as well as bilateral S2, SMA and ACC.

It is conceivable that the bottom-up activation of DLPFC induced by ASN-PES may trigger top-down responses, since ACC is implicated in the elicitation and control of sympathetic autonomic arousal. Therefore, the activation of right DLPFC by ASN may culminate in nucleous accumbens (NAc) activation in order to activate pain descending modulatory system together with PAG and rostroventral medulla (RVM; [80,81]). This pathway could explain the sense of relaxation and well being reported by subjects following the active intervention.

We observed that stimulation of right ASN produced similar results seen during VN stimulation with electrodes and implanted devices [46]. During that study, fMRI images showed ipsilateral activation of nucleus of solitary tract (NST), which is the primary central relay of vagal afferents, insula, thalamus, caudate nucleus and SSC; deactivation occurred in hippocampus, contralateral NST and ipsilateral spinal TN. In a subsequent period, activation was observed in substantia nigra, ventral tegmental area (VTA), dorsal raphe nuclei (DRN) and PAG. Based on our findings, we cannot affirm that the ASN-PES involves the activation of subcortical areas, but the anatomical correlation of ASN and VN raises an intriguing question to be explored in future studies. The anatomical structure of ASN gives us biological support to investigate the ASN-PES as a more accessible alternative for routine clinical use when therapeutic approach is to target the VN.

Also, a better comprehension of ASN-PES effect as a bottom-up neuromodulatory approach is its potential to be combined with other top-down NIBS techniques, such as transcranial direct current stimulation (tDCS) and TMS. The argument to support this question is a potential additive effect and, consequently, a better clinical response. A previous study that applied tDCS together with PES over the median nerve found increase in MEP

compared to baseline in TMS parameters [82]. Other study showed frequency-dependent motor cortex response with combined TMS and PES to test bi-directional plasticity [83]. Combined PES and tDCS intervention on patients with chronic low back pain improved symptoms than either intervention alone or sham in another trial [84]. In addition, a systematic review on stimulus parameters of PES in healthy subjects demonstrated that higher intensities of stimulation produced more consistent effects on the increase in excitability of the corticomotor pathway [10]. In another study, IMS [which appears to encompass the same type of stimulus as EA [85]] enhanced inhibitory modulation in cortical and infracortical pain processing systems when applied to women with knee osteoarthritis undergoing tDCS [37]. Possibly, modulatory techniques such as NIBS and PES attempt to re-reorganize neural circuits, improving malfunction of the whole system on cortical, infracortical, spinal and local sites.

## Study Limitations

It is necessary to point out some limitations concerning this study. We did not have a 3D device to confirm the probe location to relate it to Brodmann's areas. Instead, we used the 10/10 International System, as shown in Table 1. Likewise, we did not have short distance inter-probes, which would have helped to control noise data from skin blood flow, although we did not place probes in the forehead [86]. Scalp hemodynamics often contaminates fNIRS signals, and standard source-detector distance channels tend to over-estimate the artifacts [87]. These limitations interfere with the evaluation of cortical activation. Actually, fNIRS technical limitations include superficial depth cortical evaluation, cardiovascular frequency noise, environmental light noise and motion artifacts [56,57,75]. Furthermore, as it was already pointed out, a single-session of unilateral electrical stimulation of a craniocervical nerve can tell us about its acute manifestations without temporal changes, that can be different in subsequent measurements, as pointed out by other authors [16,46,64].

While a physiological basis study on cortical responses, we must consider the amostral design that included only right ASN

stimulation in healthy, right-handed males in a controlled environment. As expected, we observed large inter-individual responses, which might be due to a particular cortical organization or anatomical features, such as skull and subcutaneous tissues thickness, head format and skin or hair pigmentation [19]. Variables such as tiredness, stress, muscular tension, anxiety, expectancy, fear of pain, discomfort due to sitting still or cap pressure can change mental status, which can activate unexpected areas; this may be the reason why sham procedure data showed more variability than active stimulation data. Females were not included in our study to avoid hormonal influences on results, as women are more susceptible to negative emotional responses such as fear of pain, stress and anxiety [88]. The exclusion of females may generate either better or worse cortical responses to stimulation. Response patterns may also be different with bilateral stimulation in healthy vs. chronic pain patients. Other variables, such as age, lifestyle, education level, genetics and even recent news about chronobiology may play a fundamental role on response patterns in other subgroups that experience top-down or bottom-up modulations [89,90].

Moreover, we observed that studies related to PES are very heterogeneous with unstandardized nomenclature, protocols, electrical features, duration and type of stimulus [10-12]. It is necessary to develop an academic consensus aiming to standardize research and clinical protocols since PES techniques seem to be a promising therapeutic tool for pain management and neuro-rehabilitation.

## Conclusions

In conclusion, cortical activation of sensorimotor and DLPFC induced by non-painful ASN-PES seems to activate the same crucial pain cortical related areas, acting on bottom-up modulation pathway. Also, it opens a novel window of research into the possibilities of ASN-PES on modulation for treatment purposes. Further studies are needed in order to explore this technique as a potential therapeutic tool and its impact in clinical settings.

## References


1. Melzack R. Pain and the neuromatrix in the brain. J. Dent. Educ. 2001; 65: 1378–1382.
2. Chapman CR, Tuckett RP, Song CW. Pain and stress in a systems perspective: reciprocal neural, endocrine, and immune interactions. J. Pain. 2008; 9: 122–145.
3. Ong WY, Stohler CS, Herr DR. Role of the prefrontal cortex in pain processing. Mol. Neurobiol. 2019; 56: 1137–1166.
4. Wiech K, Ploner M, Tracey I. Neurocognitive aspects of pain perception. Trends Cogn. Sci. 2008; 12: 306–313.
5. O'Connell NE, Wand BM, Marston L, Spencer S, Desouza LH. Non-invasive brain stimulation techniques for chronic pain. Cochrane Database Syst. Rev. 2010; 9: CD008208.
6. Leite J, Carvalho S, Battistella LR, Caumo W, Fregni F. Editorial: the role of primary motor cortex as a marker for and modulator of pain control and emotional-affective processing. Front. Hum. Neurosci. 2017; 11: 270.
7. Ohara PT, Vit JP, Jasmin L. Cortical modulation of pain. Cell. Mol. Life Sci. 2005; 62: 44–52.
8. Hadjipavlou G, Dunckley P, Behrens TE, Tracey I. Determining anatomical connectivities between cortical and brainstem pain processing regions in humans: a diffusion tensor imaging study in healthy controls. Pain. 2006; 123: 169–178.
9. Yaksh TL, Luo ZD. Anatomy of the pain processing system. In: SD Waldman, editor. Interventional Pain Management, 2nd edn. Philadelphia: Elsevier. 2007; 11–20.
10. Chipchase LS, Schabrun SM, Hodges PW. Peripheral electrical stimulation to induce cortical plasticity: a systematic review of stimulus parameters. Clin. Neurophysiol. 2011; 122: 456–463.
11. Rossini PM, Burke D, Chen R, Cohen LG, Daskalakis Z, et al. Non-invasive electrical and magnetic stimulation of the brain, spinal cord, roots and peripheral nerves: basic principles and procedures for routine clinical and research application. An updated report from an I.F.C.N. committee. Clin. Neurophysiol. 2015; 126: 1071–1107.

12. Chakravarthy K, Nava A, Christo PJ, Williams K. Review of recent advances in peripheral nerve stimulation (PNS). Curr. Pain Headache Rep. 2016; 20: 60.
13. Sandkühler J. Learning and memory in pain pathways. Pain. 2000; 88: 113–118.
14. Jiang Y, Wang H, Liu Z, Dong Y, Dong Y, et al. Manipulation of and sustained effects on the human brain induced by different modalities of acupuncture: an fMRI study. PLoS One. 2013; 8: e66815.
15. Zhang R, Lao L, Ren K, Berman BM. Mechanisms of acupuncture-electroacupuncture on persistent pain. Anesthesiology. 2014; 120: 482–503.
16. Tanosaki M, Hoshi Y, Iguchi Y, Oikawa Y, Oda I, et al. Variation of temporal characteristics in human cerebral hemodynamic responses to electric median nerve stimulation: a near-infrared spectroscopic study. Neurosci. Lett. 2001; 316: 75–78.
17. Tanosaki M, Sato C, Shimada M, Iguchi Y, Hoshi Y. Effect of stimulus frequency on human cerebral hemodynamic responses to electric median nerve stimulation: a near-infrared spectroscopic study. Neurosci. Lett. 2003; 352: 1–4.
18. Franceschini MA, Fantini S, Thompson JH, Culver JP, Boas DA. Hemodynamic evoked response of the sensorimotor cortex measured noninvasively with near-infrared optical imaging. Psychophysiology. 2003; 40: 548–560.
19. Niederhauser BD, Rosenbaum BP, Gore JC, Jarquin-Valdivia AA. A functional near-infrared spectroscopy study to detect activation of somatosensory cortex by peripheral nerve stimulation. Neurocrit. Care. 2008; 9: 31–36.
20. Takeuchi M, Hori E, Takamoto K, Tran AH, Satoru K, et al. Brain cortical mapping by simultaneous recording of functional near infrared spectroscopy and electroencephalograms from the whole brain during right median nerve stimulation. Brain Topogr. 2009; 22: 197–214.
21. Hu SV, Caicedo A, Bruley DF, Harrison Editors, DK. Oxygen Transport to Tissue XXXVI. Vol. 812. Springer, New York: Springer Science+Business Media. 2014.
22. Muthalib M, Ferrari M, Quaresima V, Kerr G, Perrey S. Functional near-infrared spectroscopy to probe sensorimotor region activation during electrical stimulation-evoked

movement. Clin. Physiol. Funct. Imaging. 2018; 38: 816–822.
23. Blickenstorfer A, Kleiser R, Keller T, Keisker B, Meyer M, et al. Cortical and subcortical correlates of functional electrical stimulation of wrist extensor and flexor muscles revealed by fMRI. Hum. Brain Mapp. 2009; 30: 963–975.
24. Lee CH, Sugiyama T, Kataoka A, Kudo A, Fujino F, et al. Analysis for distinctive activation patterns of pain and itchy in the human brain cortex measured using near infrared spectroscopy (NIRS). PLoS One. 2013; 8: e75360.
25. Muthalib M, Re R, Zucchelli L, Perrey S, Contini D, et al. Effects of increasing neuromuscular electrical stimulation current intensity on cortical sensorimotor network activation: a time domain fNIRS study. PLoS One. 2015; 10: e0131951.
26. Aasted CM, Yücel MA, Steele SC, Peng K, Boas DA, et al. Frontal lobe hemodynamic responses to painful stimulation: a potential brain marker of nociception. PLoS One. 2016; 11: e0165226.
27. Becerra L, Harris W, Grant M, George E, Boas D, et al. Diffuse optical tomography activation in the somatosensory cortex: specific activation by painful vs. non-painful thermal stimuli. PLoS One. 2009; 4: e8016.
28. Becerra L, Harris W, Joseph D, Huppert T, Boas DA, et al. Diffuse optical tomography of pain and tactile stimulation: activation in cortical sensory and emotional systems. Neuroimage. 2008; 41: 252–259.
29. Yücel MA, Aasted CM, Petkov MP, Borsook D, Boas DA, et al. Specificity of hemodynamic brain responses to painful stimuli: a functional near-infrared spectroscopy study. Sci. Rep. 2015; 5: 9469.
30. Seo SY, Lee KB, Shin JS, Lee J, Kim MR, et al. Effectiveness of acupuncture and electroacupuncture for chronic neck pain: a systematic review and meta-analysis. Am. J. Chin. Med. 2017; 45: 1573–1595.
31. Lam M, Galvin R, Curry P. Effectiveness of acupuncture for nonspecific chronic low back pain. Spine. 2013; 38: 2124–2138.
32. Salazar AP, Stein C, Marchese RR, Plentz RD, Pagnussat AS. Electric stimulation for pain relief in patients with fibromyalgia: a systematic review and meta-analysis of

randomized controlled trials. Pain Physician. 2017; 20: 15–25.
33. de Graca-Tarragó M, Deitos A, Patrícia Brietzke A, Torres ILS, Cadore Stefani L, et al. Electrical intramuscular stimulation in osteoarthritis enhances the inhibitory systems in pain processing at cortical and cortical spinal system. Pain Med. 2016; 17: 877–891.
34. Couto C, de Souza IC, Torres IL, Fregni F, Caumo W. Paraspinal stimulation combined with trigger point needling and needle rotation for the treatment of myofascial pain: a randomized sham-controlled clinical trial. Clin. J. Pain. 2014; 30: 214–223.
35. Botelho L, Angoleri L, Zortea M, Deitos A, Brietzke A, et al. Insights about the neuroplasticity state on the effect of intramuscular electrical stimulation in pain and disability associated with chronic myofascial pain syndrome (MPS): a double-blind, randomized, sham-controlled trial. Front. Hum. Neurosci. 2018; 12: 388.
36. Botelho LM, Morales-Quezada L, Rozisky JR, Brietzke AP, Torres ILS, et al. A framework for understanding the relationship between descending pain modulation, motor corticospinal, and neuroplasticity regulation systems in chronic myofascial pain. Front. Hum. Neurosci. 2016; 10: 308.
37. Tarragó GM, Deitos A, Brietzke AP, Vercelino R, Torres ILS, et al. Descending control of nociceptive processing in knee osteoarthritis is associated with intracortical disinhibition. Medicine. 2016; 95: e3353.
38. Chipchase LS, Schabrun SM, Hodges PW. Corticospinal excitability is dependent on the parameters of peripheral electric stimulation: a preliminary study. Arch. Phys. Med. Rehabil. 2011; 92: 1423–1430.
39. Tan DW, Schiefer MA, Keith MW, Anderson JR, Tyler DJ. Stability and selectivity of a chronic, multi-contact cuff electrode for sensory stimulation in human amputees. J. Neural Eng. 2015; 12: 026002.
40. Ghafoor U, Kim S, Hong KS. Selectivity and longevity of peripheral-nerve and machine interfaces: a review. Front. Neurorobot. 2017; 11: 59.

41. Castillo Saavedra L, Mendonca M, Fregni F. Role of the primary motor cortex in the maintenance and treatment of pain in fibromyalgia. Med. Hypotheses. 2014; 83: 332–336.
42. Jensen MP, Day MA, Miró J. Neuromodulatory treatments for chronic pain: efficacy and mechanisms. Nat. Rev. Neurol. 2014; 10: 167–178.
43. Hachem LD, Wong SM, Ibrahim GM. The vagus afferent network: emerging role in translational connectomics. Neurosurg. Focus. 2018; 45: E2.
44. Frangos E, Ellrich J, Komisaruk BR. Non-invasive access to the vagus nerve central projections via electrical stimulation of the external ear: fMRI evidence in humans. Brain Stimul. 2015; 8: 624–636.
45. Yakunina N, Kim SS, Nam EC. Optimization of transcutaneous vagus nerve stimulation using functional MRI. Neuromodulation. 2017; 20: 290–300.
46. Frangos E, Komisaruk BR. Access to vagal projections via cutaneous electrical stimulation of the neck: fMRI evidence in healthy humans. Brain Stimul. 2017; 10: 19–27.
47. Rigo JC, Couto C, Dalla-Corte RR. Cluster headache in an elderly patient treated with neurofunctional acupuncture a case report. Acupunct. Relat. Ther. 2014; 2: 39–42.
48. Chassot M, Dussan-Sarria JA, Sehn FC, Deitos A, de Souza A, et al. Electroacupuncture analgesia is associated with increased serum brain-derived neurotrophic factor in chronic tension-type headache: a randomized, sham controlled, crossover trial. BMC Complement. Altern Med. 2015; 15: 144.
49. Chou DE, Gross GJ, Casadei CH, Yugrakh MS. External trigeminal nerve stimulation for the acute treatment of migraine: open-label trial on safety and efficacy. Neuromodulatio. 2017; 20: 678–683.
50. Waki H, Suzuki T, Tanaka Y, Tamai H, Minakawa Y, et al. Effects of electroacupuncture to the trigeminal nerve area on the autonomic nervous system and cerebral blood flow in the prefrontal cortex. Acupunct. Med. 2017; 35: 339–344.
51. Sarrazin JL, Toulgoat F, Benoudiba F. The lower cranial nerves: IX, X, XI, XII. Diagn. Interv. Imaging. 2013; 94: 1051–1062.

52. Liu HF, Won HS, Chung IH, Kim IB, Han SH. Morphological characteristics of the cranial root of the accessory nerve. Clin. Anat. 2014; 27: 1167–1173.
53. Shoja MM, Oyesiku NM, Shokouhi G, Griessenauer CJ, Chern JJ, et al. A comprehensive review with potential significance during skull base and neck operations, Part II: glossopharyngeal, vagus, accessory and hypoglossal nerves and cervical spinal nerves 1-4. Clin. Anat. 2014; 27: 131–144.
54. Benninger B, McNeil J. Transitional nerve: a new and original classification of a peripheral nerve supported by the nature of the accessory nerve (CN XI). Neurol. Res. Int. 2010; 2010: 476018.
55. Mitsuoka K, Kikutani T, Sato I. Morphological relationship between the superior cervical ganglion and cervical nerves in japanese cadaver donors. Brain Behav. 2017; 7: e00619.
56. Ferrari M, Quaresima V. A brief review on the history of human functional near-infrared spectroscopy (fNIRS) development and fields of application. Neuroimage. 2012; 63: 921–935.
57. Scholkmann F, Kleiser S, Metz AJ, Zimmermann R, Mata Pavia J, et al. A review on continuous wave functional near-infrared spectroscopy and imaging instrumentation and methodology. Neuroimage. 2014; 85: 6–27.
58. Phillips AA, Chan FHN, Zheng MMZ, Krassioukov AV, Ainslie PN. Neurovascular coupling in humans: physiology, methodological advances and clinical implications. J. Cereb. Blood Flow Metab. 2016; 36: 647–664.
59. Owen DG, Clarke CF, Ganapathy S, Prato FS, St Lawrence KS. Using perfusion MRI to measure the dynamic changes in neural activation associated with tonic muscular pain. Pain. 2010; 148: 375–386.
60. Nguyen HD, Hong KS. Bundled-optode implementation for 3D imaging in functional near-infrared spectroscopy. Biomed. Opt. Express. 2016; 7: 3491–3507.
61. Hong KS, Zafar A. Existence of initial DIP for BCI: an illusion or reality. Front. Neurorobot. 2018; 12: 69.
62. Hoshi Y. Hemodynamic signals in fNIRS. Prog. Brain Res. 2016; 225: 153–179.

63. Nguyen HD, Hong KS, Shin YI. Bundled-optode method in functional near-infrared spectroscopySakakibara. PLoS One. 2016; 11: e0165146.
64. Jang SH, Jang WH, Chang PH, Lee SH, Jin SH, et al. Cortical activation change induced by neuromuscular electrical stimulation during hand movements: a functional NIRS study. J. Neuroeng. Rehabil. 2014; 11: 29.
65. Hong KS, Bhutta MR, Liu X, Shin YI. Classification of somatosensory cortex activities using fNIRS. Behav. Brain Res. 2017; 333: 225–234.
66. Strait M, Scheutz M. What we can and cannot (yet) do with functional near infrared spectroscopy. Front. Neurosci. 2014; 8: 117.
67. Naseer N, Hong KS. fNIRS-based brain-computer interfaces: a review. Front. Hum. Neurosci. 2015; 9: 3.
68. Khan MJ, Hong MJ, Hong KS. Decoding of four movement directions using hybrid NIRS-EEG brain-computer interface. Front. Hum. Neurosci. 2014; 8: 244.
69. Hong KS, Khan MJ. Hybrid brain-computer interface techniques for improved classification accuracy and increased number of commands: a review. Front. Neurorobot. 2017; 11: 35.
70. Birkett MA, Day SJ. Internal pilot studies for estimating sample size. Stat. Med. 1994; 13: 2455–2463.
71. Kohl M, Nolte C, Heekeren HR, Horst S, Scholz U, et al. Determination of the wavelength dependence of the differential pathlength factor from near-infrared pulse signals. Phys. Med. Biol. 1998; 43: 1771–1782.
72. Zhao H, Tanikawa Y, Gao F, Onodera Y, Sassaroli A, et al. Maps of optical differential pathlength factor of human adult forehead, somatosensory motor and occipital regions at multi-wavelengths in NIR. Phys. Med. Biol. 2002; 47: 2075–2093.
73. Jurcak V, Tsuzuki D, Dan I. 10/20, 10/10, and 10/5 systems revisited: their validity as relative head-surface-based positioning systems. Neuroimage. 2007; 34: 1600–1611.
74. Koessler L, Maillard L, Benhadid A, Vignal JP, Felblinger J, et al. Automated cortical projection of EEG sensors: anatomical correlation via the international 10–10 system. Neuroimage. 2009; 46: 64–72.

75. Tak S, Chul Ye J. Statistical analysis of fNIRS data: a comprehensive review. Neuroimage. 2014; 85: 72–91.
76. Sankarasubramanian V, Cunningham DA, Potter-Baker KA, Beall EB, Roelle SM, et al. Transcranial direct current stimulation targeting primary motor versus dorsolateral prefrontal cortices: proof-of-concept study investigating functional connectivity of thalamocortical networks specific to sensory-affective information processing. Brain Connect. 2017; 7: 182–196.
77. Lorenz J, Minoshima S, Casey KL. Keeping pain out of mind: the role of the dorsolateral prefrontal cortex in pain modulation. Brain. 2003; 126: 1079–1091.
78. Cieslik EC, Zilles K, Caspers S, Roski C, Kellermann TS, et al. Is there one DLPFC in cognitive action control? Evidence for heterogeneity from co-activation-based parcellation. Cereb. Cortex. 2013; 23: 2677–2689.
79. Brasil-Neto JP. Motor cortex stimulation for pain relief: do corollary discharges play a role? Front. Hum. Neurosci. 2016; 10: 323.
80. Navratilova E, Porreca F. Reward and motivation in pain and pain relief. Nat. Neurosci. 2014; 17: 1304–1312.
81. Elman I, Borsook D. Perspective common brain mechanisms of chronic pain and addiction. Neuron. 2016; 89: 11–36.
82. Rizzo V, Terranova C, Crupi D, Sant'angelo A, Girlanda P, et al. Increased transcranial direct current stimulation after effects during concurrent peripheral electrical nerve stimulation. Brain Stimul. 2014; 7: 113–121.
83. Pitcher JB, Ridding MC, Miles TS. Frequency-dependent, bi-directional plasticity in motor cortex of human adults. Clin. Neurophysiol. 2003; 114: 1265–1271.
84. Schabrun SM, Jones E, Elgueta Cancino EL, Hodges PW. Targeting chronic recurrent low back pain from the top-down and the bottom-up: a combined transcranial direct current stimulation and peripheral electrical stimulation intervention. Brain Stimul. 2014; 7: 451–459.
85. Kim TH, Lee CR, Choi TY, Lee MS. Intramuscular stimulation therapy for healthcare: a systematic review of randomised controlled trials. Acupunct. Med. 2012; 30: 286–290.

86. Takahashi T, Takikawa Y, Kawagoe R, Shibuya S, Iwano T, et al. Influence of skin blood flow on near-infrared spectroscopy signals measured on the forehead during a verbal Fluency task. Neuroimage. 2011; 57: 991–1002.
87. Sato T, Nambu I, Takeda K, Aihara T, Yamashita O, et al. Reduction of global interference of scalp-hemodynamics in functional near-infrared spectroscopy using short distance probes. Neuroimage. 2016; 141: 120–132.
88. da Silva NRJ, Laste G, Stefani LC, Cambraia-Canto G, Torres ILS, et al. Combined neuromodulatory interventions in acute experimental pain: assessment of melatonin and non-invasive brain stimulation. Front. Behav. Neurosci. 2015; 9: 77.
89. Cummings M, Baldry P. Regional myofascial pain: diagnosis and management. Best Pract. Res. Clin. Rheumatol. 2007; 21: 367–387.
90. Ridding MC, Ziemann U. Determinants of the induction of cortical plasticity by non-invasive brain stimulation in healthy subjects. J. Physiol. 2010; 588: 2291–2304.

## Supplementary Material

Supplementary data - HbO mean curves in each channel between groups (40 channels).

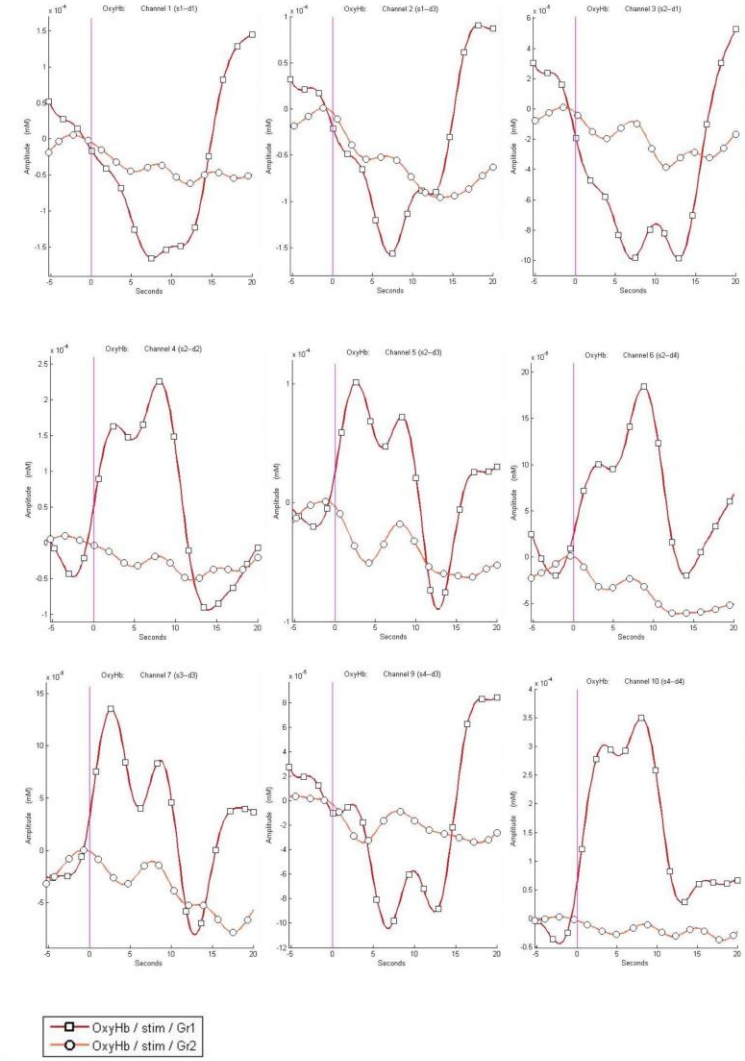

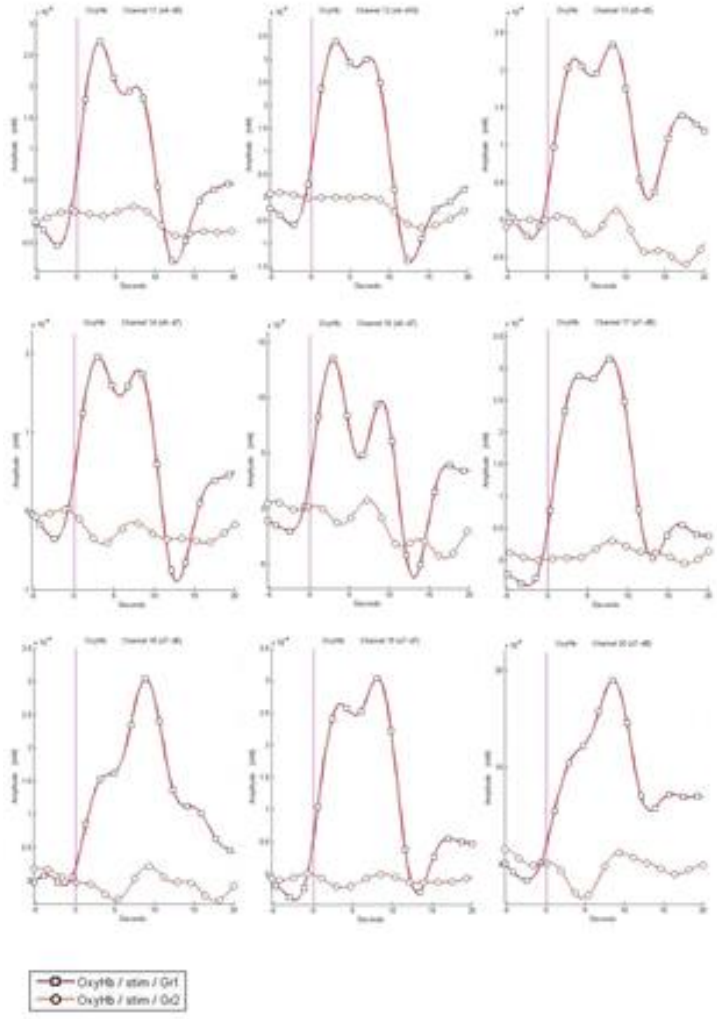
OxyHb / stim / Gr1
OxyHb / stim / Gr2

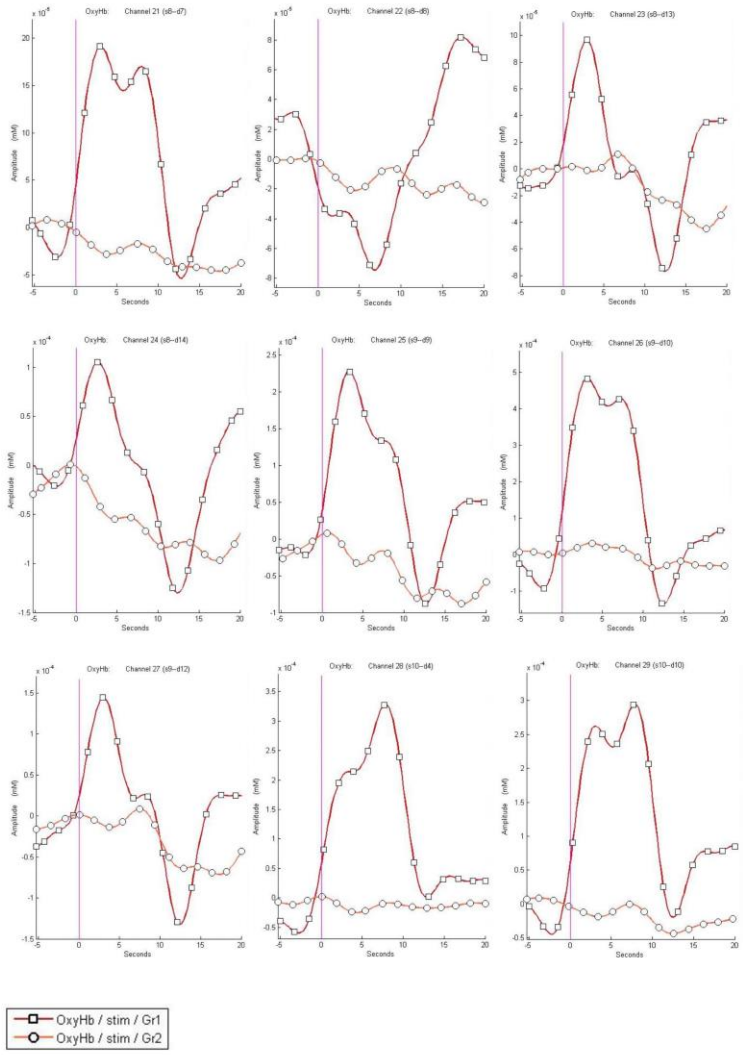
OxyHb: Channel 21 (s8–d7)
OxyHb: Channel 22 (s8–d8)
OxyHb: Channel 23 (s9–d13)
OxyHb: Channel 24 (s8–d14)
OxyHb: Channel 25 (s9–d9)
OxyHb: Channel 26 (s9–d10)
OxyHb: Channel 27 (s9–d12)
OxyHb: Channel 28 (s10–d4)
OxyHb: Channel 29 (s10–d10)
Amplitude (mM)
Seconds
OxyHb / stim / Gr1
OxyHb / stim / Gr2

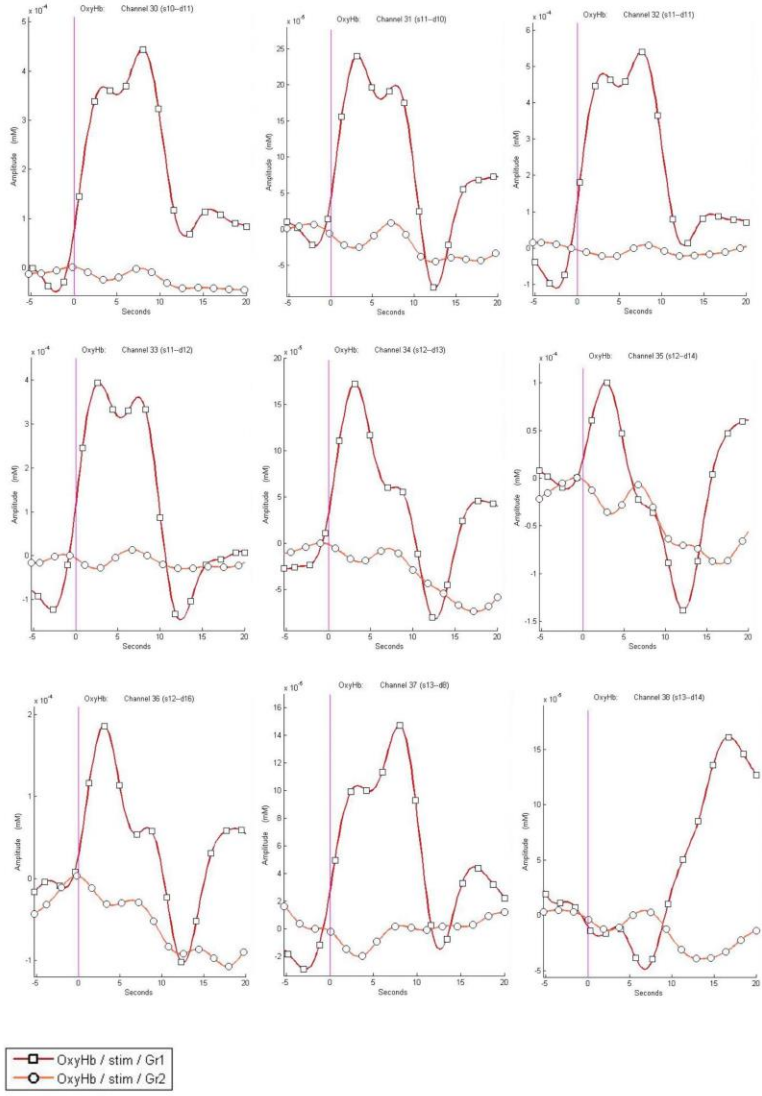
OxyHb: Channel 30 (s10–d11)
OxyHb: Channel 31 (s11–d10)
OxyHb: Channel 32 (s11–d11)
OxyHb: Channel 33 (s11–d12)
OxyHb: Channel 34 (s12–d13)
OxyHb: Channel 35 (s12–d14)
OxyHb: Channel 36 (s12–d16)
OxyHb: Channel 37 (s13–d8)
OxyHb: Channel 38 (s13–d14)
Amplitude (mM)
Seconds
OxyHb / stim / Gr1
OxyHb / stim / Gr2

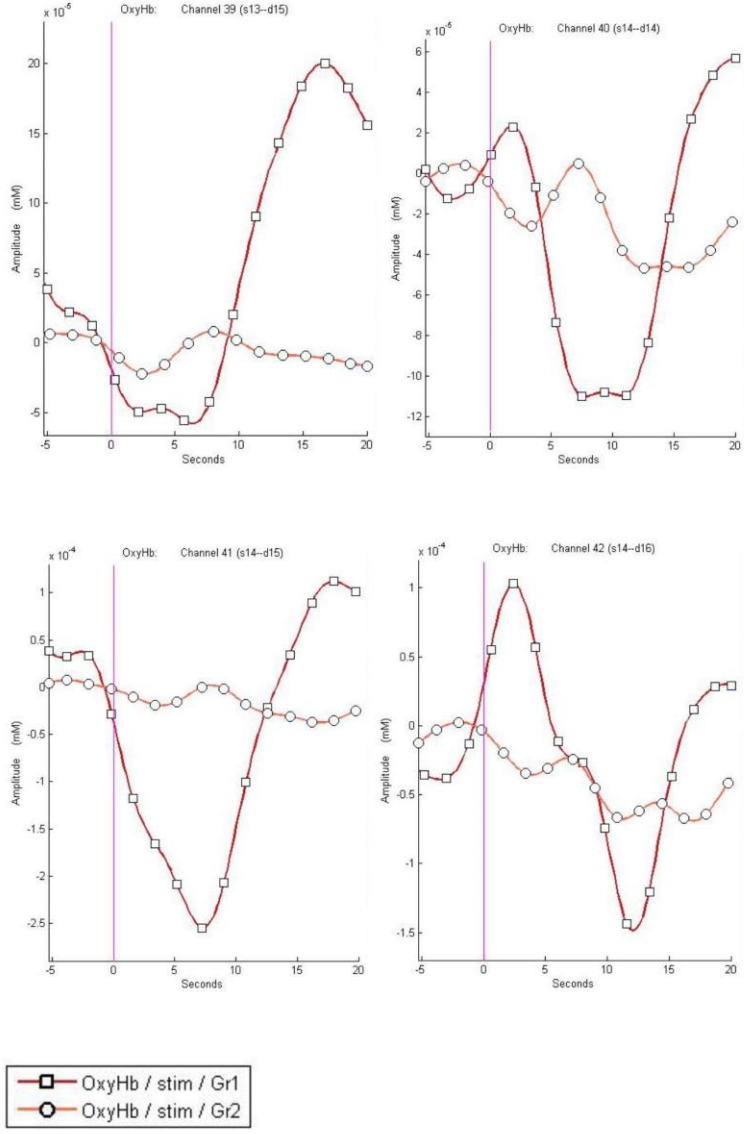
x 10^-6
OxyHb: Channel 39 (s13--d15)
Amplitude (mM)
Seconds
x 10^-6
OxyHb: Channel 40 (s14--d14)
Amplitude (mM)
Seconds
x 10^-4
OxyHb: Channel 41 (s14--d15)
Amplitude (mM)
Seconds
x 10^-4
OxyHb: Channel 42 (s14--d16)
Amplitude (mM)
Seconds
OxyHb / stim / Gr1
OxyHb / stim / Gr2